

# VARIABLE BANDWIDTH MEAN SHIFT FOR SMOOTHING ULTRASONIC IMAGES

*Thomas Grenier, Chantal Revol-Muller, Franck Davignon, Olivier Basset, Gérard Gimenez*

CREATIS, CNRS UMR 5515, Inserm U 630  
Bât. B. Pascal, 69621 Villeurbanne, France

phone: + (33) 472 43 81 91, fax: + (33) 472 43 85 26, email: chantal.muller@creatis.insa-lyon.fr  
web: www.creatis.insa-lyon.fr

## ABSTRACT

As the variance of the statistics of ultrasonic data in a homogeneous tissue may be rather large and the statistics of different tissues may be very similar, a new filtering approach is proposed to enhance the contrast in ultrasonic images. It is based on the Variable Bandwidth Mean Shift algorithm adapted to the specificities of ultrasonic data. A fully automatic adaptive bandwidth selection in both range and spatial domains is described. Our method was compared to a Variable Bandwidth Mean Shift algorithm based on an adaptive range scale selection and a fixed spatial scale parameter. The results show the superiority of our method.

## 1. INTRODUCTION

Ultrasonic images are characterised by a relatively poor quality and thus, processing such as automatic segmentation is a difficult problem [1], [2]. The image degradation includes primarily the speckle noise, the blurring of spatial information perpendicular to the propagation direction of ultrasonic waves, and the non-constant attenuation of ultrasound. Although dynamic focusing techniques are used, the lateral resolution is poor and the structures are blurred in a direction perpendicular to the ultrasonic propagation. In most cases, the structures to be detected, such as tumours, have acoustic characteristics similar to the surrounding tissues. Thus, the contrast between the various tissues is poor. This makes the determination of an accurate border difficult. The attenuation of ultrasound depends on the nature of the investigated tissues. Consequently, a homogeneous tissue does not appear quite homogeneous on the image. It may be visualised with a slight variation of intensity in the ultrasonic propagation direction, despite the correction of the Time Gain Compensation, which is constant and independent of the nature of tissues. Moreover, the principle of image formation uses the focalisation of the ultrasonic beam. Then, the lateral resolution in the image, defined by the resolution cell size, is not constant along the propagation direction. It also implies variations in the statistics of a homogeneous tissue at different depth of the tissue.

As the variance of the statistics in a homogeneous tissue may be rather large and the statistics of different tissue may be very similar, several filtering techniques are proposed in the literature to enhance the contrast in ultrasonic data.

The most widely used techniques for reducing the speckle noise are the spatial or frequency compounding that consist in averaging uncorrelated data. Several filtering techniques have also been described. They are summarized in [3].

More recently, anisotropic diffusion techniques have been adapted to the spatial properties of speckle to enhance the contrast in ultrasonic images [4]. The Mean Shift analysis has shown its efficiency to achieve a high quality discontinuity-preserving filtering by identifying local modes of the underlying distribution in the joint spatial-range domain [5]. We propose in this paper a Variable Bandwidth Mean Shift filtering based on an automated bandwidth selection both in range and spatial domains (VBMS R+S). This technique associates to each data point a range scale parameter computed from the data points and a spatial scale parameter obtained from the a priori knowledge about the resolution of the ultrasound probe.

## 2. ULTRASONIC IMAGES

In order to evaluate the efficiency of our method, we have simulated data using the Field software developed by J.A. Jensen [6]. Given the positions and the acoustical characteristics of the scatterers and also the beam characteristics, the software is able to compute the emitted and received waves, thus creating the corresponding RF signals. The numerical phantoms consist in a 60 mm depth, 30 mm wide, 10 mm thick scattering medium with 100.000 randomly disposed scatterers with Gaussian-distributed amplitudes. In the Field software, the acoustic characteristics of each scatterer in the simulated tissue are defined through the parameter called "amplitude". This parameter controls the echogenicity of the medium. A 10 mm diameter cylindrical inclusion is placed at the centre of the phantom. The amplitude inside is set to 0.1, the amplitude outside is set to 1. The geometry of the two-region phantom is shown in Fig. 1.

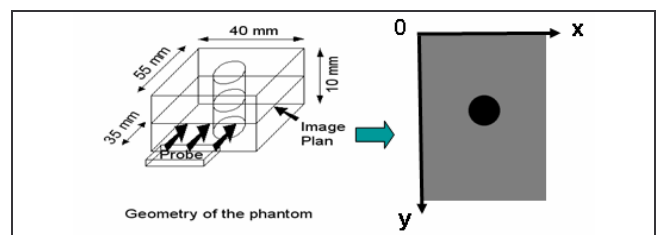


Figure 1: Geometry of the phantom

The simulation is computed using a 3.5MHz array probe with a focal zone centred on the inclusion in reception. We used 50 RF lines sampled at a 100MHz rate. The output is then a 50\*7160 data file. For each line, the envelope of the signal is detected. The axial resolution being 0.8 mm (about 100 pixels), the envelope data was decimated by 20, thus giving a 50\*358 data file.

The lateral resolution is related to the Point Spread Function (PSF) of the imaging system. The Fig.2 (right) shows the evolution of the PSF with the depth (on the y-axis). It is obtained by placing 0.5 mm spaced scatterers along the y axis and by computing the response of the imaging system via the Field software. From the lateral profile of the PSF (in the x-axis), we consider the lateral resolution at each depth as the width at half maximum of the profile.

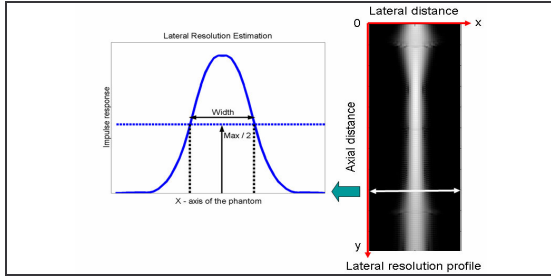


Figure 2: Lateral resolution profile of the probe

### 3. VARIABLE BANDWIDTH MEAN SHIFT

Mean shift is a non parametric estimator of density gradient developed by Fukunaga and Hostetler thirty years ago [7] and recently exploited in low level computer vision tasks by Comaniciu and Meer [5, 8]. Mean shift framework is interesting because it can take into account jointly both spatial information (pixel location in the spatial domain  $\mathbb{R}^s$ ) and range information (grey level, colour or spectral information in the range domain  $\mathbb{R}^r$ ). The resulting spatial-range domain is represented by a d-dimensional Euclidian space  $\mathbb{R}^d$ , where  $d = s + r$ . Moreover, mean shift technique is attractive, since it needs no prior knowledge on the underlying distribution of the intensities of the pixels. But its main drawback is the selection of a scale parameter tied to the joint spatial-range domain. In [9], the authors proposed a Variable Bandwidth Mean Shift procedure based on an adaptive Range scale parameter (VBMS R) and demonstrated its superiority over the fixed bandwidth density estimation methods.

In this paper, we propose a Variable Bandwidth Mean Shift filtering based on a fully adaptive bandwidth selection both in Range and Spatial domains (VBMS R+S). One novelty of our method is to take into account a priori knowledge about ultrasonic imaging such as the lateral variation of resolution.

#### 3.1 Principle of variable bandwidth mean shift

The mean shift procedure was fully described in [8, 9]. It consists in detecting the stationary points of the underlying density function, i.e. the modes of the density. In this section, we remind the general principle and the main equations governing the method. Mean shift is a non parametric method based on the kernel density estimation. The multivariate kernel density estimator with kernel K (a

radially symmetric, non-negative function centred at zero and integrating to one) and a fixed symmetric, positive definite bandwidth matrix  $\mathbf{H}$  is defined in eq. 1 for a set of n data points  $\{\mathbf{x}_i\}_{i=1,\dots,n}$  in a d-dimensional Euclidian space  $\mathbb{R}^d$ .

$$\hat{f}(\mathbf{x}) = \frac{1}{n} \sum_{i=1}^n K_{\mathbf{H}}(\mathbf{x} - \mathbf{x}_i) \quad (1)$$

The terminology "fixed bandwidth" means that the density at each point  $\mathbf{x}$  is estimated using the same scaled kernel over the whole data points. The limitations of the fixed bandwidth kernel based estimation are an undersmoothing effect at the tails and an oversmoothing effect at the peaks of the density. The performance also decreases when the data exhibit local scale variations like in ultrasonic imaging.

An improvement of the method is to make the bandwidth matrix  $\mathbf{H}$  variable. One solution is to define a bandwidth matrix  $\mathbf{H}_i$  for each data point  $\mathbf{x}_i$ ,  $i = 1, \dots, n$ . The resulting multivariate estimator is called the sample point density estimator given by eq. 2 and has proved its efficiency over the fixed bandwidth estimator [9].

$$\hat{f}(\mathbf{x}) = \frac{1}{n} \sum_{i=1}^n K_{\mathbf{H}_i}(\mathbf{x} - \mathbf{x}_i) \quad (2)$$

The bandwidth  $\mathbf{H}_i$  scales the kernel support to be radial symmetric.

$$K_{\mathbf{H}_i}(\mathbf{u}) = (\det[\mathbf{H}_i])^{-\frac{1}{2}} \cdot K\left(\mathbf{H}_i^{-\frac{1}{2}} \mathbf{u}\right) \quad (3)$$

In our application, we will restrict  $\mathbf{H}_i$  to a diagonal matrix. Each element  $h_{i,m}$  ( $m = 1, \dots, d$ ) of the matrix is the scale parameter of the m<sup>th</sup> dimension of the d-dimensional Euclidian space  $\mathbb{R}^d$ . Due to its symmetry property,  $K(\mathbf{u})$  can be replaced by its profile  $k : [0, \infty) \rightarrow \mathbb{R}$ , a monotonically decreasing function

$$K(\mathbf{u}) = c_{k,d} \cdot k(\mathbf{u}^T \mathbf{u}) \quad \text{with} \quad \begin{cases} k(u) \geq 0 & \text{for } 0 \leq u \leq 1 \\ k(u) = 0 & \text{for } u > 1 \end{cases} \quad (4)$$

where  $c_{k,d}$  is a normalization constant.

Eq. 2 can be rewritten taking into account eq. 3 and eq. 4

$$\begin{aligned} \hat{f}(\mathbf{x}) &= \frac{c_{k,d}}{n} \sum_{i=1}^n (\det[\mathbf{H}_i])^{-\frac{1}{2}} \cdot k\left(\left(\mathbf{x} - \mathbf{x}_i\right)^T \cdot \mathbf{H}_i^{-1} \cdot \left(\mathbf{x} - \mathbf{x}_i\right)\right) \\ &= \frac{c_{k,d}}{n} \sum_{i=1}^n (\det[\mathbf{H}_i])^{-\frac{1}{2}} \cdot k\left(d[\mathbf{x}, \mathbf{x}_i, \mathbf{H}_i]^2\right) \end{aligned} \quad (5)$$

where  $d[\mathbf{x}, \mathbf{x}_i, \mathbf{H}_i]^2$  denotes the square Mahalanobis distance from  $\mathbf{x}$  to  $\mathbf{x}_i$ .

Using the linearity property of eq. 5, the density gradient estimator is obtained as the gradient of the density estimator in eq. 6.

$$\begin{aligned} \hat{\nabla} f(\mathbf{x}) &\equiv \nabla \hat{f}(\mathbf{x}) \\ &= \frac{2c_{k,d}}{n} \sum_{i=1}^n (\det[\mathbf{H}_i])^{-\frac{1}{2}} \cdot \mathbf{H}_i^{-1} \cdot (\mathbf{x} - \mathbf{x}_i) \cdot k'\left(d[\mathbf{x}, \mathbf{x}_i, \mathbf{H}_i]^2\right) \end{aligned} \quad (6)$$

This expression can be rewritten with the notation  $\mathbf{Q}_i(\mathbf{x})$  defined in eq. 7, where we note  $g(u) = -k'(u)$ .

$$\mathbf{Q}_i(\mathbf{x}) = (\det[\mathbf{H}_i])^{-\frac{1}{2}} \cdot \mathbf{H}_i^{-1} \cdot g\left(d[\mathbf{x}, \mathbf{x}_i, \mathbf{H}_i]^2\right) \quad (7)$$

$$\hat{\nabla} f(\mathbf{x}) = \frac{2c_{k,d}}{n} \left( \sum_{i=1}^n \mathbf{Q}_i(\mathbf{x}) \right) \left[ \left( \sum_{i=1}^n \mathbf{Q}_i(\mathbf{x}) \right)^{-1} \sum_{i=1}^n \mathbf{Q}_i(\mathbf{x}) \cdot \mathbf{x}_i - \mathbf{x} \right] \quad (8)$$

The mean shift vector  $M(\mathbf{x})$  is defined in eq. 9. It was shown that this vector is an estimator of the normalized gradient of the underlying distribution.

$$M(\mathbf{x}) = \left( \sum_{i=1}^n \mathbf{Q}_i(\mathbf{x}) \right)^{-1} \sum_{i=1}^n \mathbf{x}_i \cdot \mathbf{Q}_i(\mathbf{x}) - \mathbf{x} \quad (9)$$

The main property of this estimator is the convergence associated with its repetitive computation. The mean shift procedure consists in an iterative computation of the mean shift vector  $M(\mathbf{x})$  and the translation of the kernel by  $M(\mathbf{x})$ . It was proved that this process converges at a point where the estimate has zero gradient i.e.  $\|M(\mathbf{x})\| \approx 0$ .

Starting from a point  $\mathbf{x} = \mathbf{x}^{[1]}$ , the successive locations of the kernel are stored by the sequence  $\{\mathbf{x}^{[l]}\}_{l=1,2,\dots}$  given by eq. 10.

$$\mathbf{x}^{[l+1]} = \left( \sum_{i=1}^n \mathbf{Q}_i(\mathbf{x}^{[l]}) \right)^{-1} \cdot \left( \sum_{i=1}^n \mathbf{x}_i \cdot \mathbf{Q}_i(\mathbf{x}^{[l]}) \right) \quad (10)$$

At each iteration,  $\|M(\mathbf{x})^{[l+1]}\| = \|\mathbf{x}^{[l+1]} - \mathbf{x}^{[l]}\|$  is evaluated. The process stops when the module of the mean shift vector is less than a tolerance threshold. The point of convergence  $\mathbf{x}_{CONV}$  corresponds to a mode of the distribution.

### 3.2 Adaptive bandwidth selection

A variable bandwidth matrix  $\mathbf{H}_i$  is determined for each data points  $\{\mathbf{x}_i\}_{i=1,\dots,n}$ . In our application, bi-dimensional images of grey levels were considered, so the spatial dimension  $s$  is equal to 2 and the range dimension  $r$  is equal to 1. The variable bandwidth matrix is expressed in eq. 11.

$$\mathbf{H}_i = \begin{bmatrix} h_{i,s1}^2 & 0 & 0 \\ 0 & h_{i,s2}^2 & 0 \\ 0 & 0 & h_{i,r}^2 \end{bmatrix} \quad (11)$$

Due to the different nature of the spatial and the range spaces, a method for the bandwidth selection is defined for each space:

- the spatial scale parameters  $h_{i,s1}$  and  $h_{i,s2}$  are chosen in order to fit to the local spatial resolution of the image.
- the range scale parameter  $h_{i,r}$  derives from a property of the sample point estimator.

#### 3.2.1 Adaptive spatial bandwidths $h_{i,s1}$ and $h_{i,s2}$

In the mean shift procedure, the use of variable spatial scale parameters is well connected to a multiscale analysis of the data. In [9], the authors propose a semi-parametric selection of the spatial parameter based on an interesting property of the mean shift vector. This solution is particularly well appropriated when nothing is known about the spatial scale of the image. In the context of ultrasonic imaging, we take benefit of additional information such as the spatial resolution of the probe. As explained in Section 2, the lateral spatial resolution of the probe is experimentally estimated for each pixel. As the spatial scale is closely related to the resolution, we assign the spatial bandwidths  $h_{i,s1}$  and  $h_{i,s2}$  using the estimated resolution of the considered pixel. To obtain  $h_{i,s2}$ , we multiply  $h_{i,s1}$  by a scalar in order to take into account the anisotropy of the image ( $h_{i,s2} = 5,2 h_{i,s1}$ ).

#### 3.2.2 Adaptive range bandwidth $h_{i,r}$

We derive the method given in [9] for computing the adaptive range scale parameter  $h_{i,r}$  for each pixel  $\{\mathbf{x}_i\}_{i=1,\dots,n}$ .

This method is based on an attractive property of the sample point estimator, which ensures a minimization of the bias

error for a particular choice of  $h_{i,r}$ . The expression of  $h_{i,r}$  is given by eq. 12.

$$h_{i,r} = h_0 \cdot \left[ \frac{\lambda}{\tilde{f}(\mathbf{x}_i)} \right]^{\frac{1}{2}} \quad (12)$$

It involves the estimation of  $f(\mathbf{x}_i)$  from the data, called pilot distribution  $\tilde{f}(\mathbf{x}_i)$ , and the determination of two constants  $h_0$  and  $\lambda$ .  $h_0$  is a fixed bandwidth computed from the one-dimensional plug-in rule proposed in [10]. According to the authors in [9], this plug-in is the best of the currently available data-driven methods for bandwidth selection.  $\lambda$  is computed from  $\{\tilde{f}(\mathbf{x}_i)\}$  usually as the geometric mean. It is a reference value which sorts the range of density values in low and high densities. When the local density is low, i.e.  $\tilde{f}(\mathbf{x}_i) < \lambda$ ,  $h_{i,r}$  increases relatively to  $h_0$  implying more smoothing for the point  $\mathbf{x}_i$ . On the contrary, when  $\tilde{f}(\mathbf{x}_i) > \lambda$ ,  $h_{i,r}$  becomes narrower. The pilot density  $\tilde{f}(\mathbf{x}_i)$  is computed for each pixel from a kernel density estimator, using a fixed range bandwidth  $h_0$  and variable spatial bandwidths  $h_{i,s1}$  and  $h_{i,s2}$  previously determined. Then, the adaptive range bandwidth  $h_{i,r}$  is determined according to eq. 12 using spatial scale parameters  $h_{i,s1}$  and  $h_{i,s2}$ .

### 3.3 Adaptive smoothing

Let  $\{\mathbf{x}_i\}_{i=1,\dots,n}$  and  $\{\mathbf{y}_i\}_{i=1,\dots,n}$  be the d-dimensional original image and the filtered points in the spatial-range domain. The mean shift filtering is obtained by applying the variable bandwidth mean shift procedure to each pixel  $\{\mathbf{x}_i\}_{i=1,\dots,n}$  of the original image and by assigning to each pixel  $\{\mathbf{y}_i\}_{i=1,\dots,n}$  of the filtered image the components of the point of convergence  $\mathbf{x}_{CONV_i}$  associated to  $\mathbf{x}_i$ .

#### Algorithm:

The adaptive smoothing was applied to bi-dimensional grey level images. Given  $\{\mathbf{x}_i\}_{i=1,\dots,n}$ :

- Compute  $h_0$  the optimal fixed range bandwidth with the plug-in rule.
- For each  $\{\mathbf{x}_i\}$ :
  - Assign the spatial bandwidths  $h_{i,s1}$  and  $h_{i,s2}$  using the lateral profile of the ultrasound probe.
  - Compute the pilot density  $\tilde{f}(\mathbf{x}_i)$  using the local spatial scales  $h_{i,s1}$ ,  $h_{i,s2}$  and compute  $\lambda_i$  with  $\log \lambda_i = n^{-1} \sum_{i=1}^n \log \tilde{f}(\mathbf{x}_i)$
  - Compute  $h_{i,r}$  given by eq. 12 using the local spatial scales  $h_{i,s1}$  and  $h_{i,s2}$ .
- For each  $\{\mathbf{x}_i\}$ , run the adaptive mean shift procedure.
- For each  $\{\mathbf{y}_i\}$ , assign  $\mathbf{y}_i = \mathbf{x}_{CONV_i}$ .

## 4. RESULTS AND DISCUSSION

We applied our method (VBMS R+S) to simulated ultrasonic data. The original image and its related grey levels distribution is displayed in Fig. 3a and Fig. 3c. We can see from the distribution that both the dark and the bright classes are indistinguishable. We compared (VBMS R+S) to a VBMS algorithm based on an adaptive range

scale parameter and fixed spatial bandwidths (VBMS R). Both algorithms used the same expression given by eq. 12 for the computation of  $h_{i,r}$ . However, in our method,  $h_{i,r}$  was determined from the data points included in the adaptive spatial bandwidths  $h_{i,s1}$  and  $h_{i,s2}$ . The fixed spatial bandwidth  $h_{s1}$  was fixed to the average lateral resolution of the probe and the same previous factor of anisotropy ( $h_{s2} = 5,2 h_{s1}$ ) was applied for deducing  $h_{s2}$ . The resulting filtered images can be observed in Fig. 3d for (VBMS R) and in Fig. 3g for (VBMS R+S). The related grey levels distributions are displayed in Fig. 3f and Fig. 3i. In Fig. 3f, it appears that (VBMS R) has slightly grouped the data points around several modes, but those modes are too numerous. (VBMS R+S) has given better results than (VBMS R), since the dark area is well isolated in the distribution of the filtered image. More data points have converged towards fewer modes. The homogeneity of the original image and the filtered images is evaluated by a thresholding. Whereas a manual thresholding is needed for the original image and the (VBMS R) filtered image (since classes are not distinguishable), an automated thresholding can detect the separation between the dark and the bright classes in (VBMS R+S) filtered image. In Fig. 3h, the resulting binary image is quite satisfying.

## 5. CONCLUSION

We have developed a Variable Bandwidth Mean Shift filtering based on both spatial and range adaptive bandwidths. For each data point, a range bandwidth was computed from the data and spatial bandwidths were determined from the lateral resolution of the ultrasound probe. Our method has shown its superiority relatively to the Variable Bandwidth Mean Shift filtering using fixed spatial scale parameters. The proposed method has several advantages on classical VBMS. First, it does not require any setting of parameter. Then, it is able to fit to the variable resolution of the ultrasound probe.

## REFERENCES

- [1] E. A. Ashton and K. J. Parker, "Multiple resolution bayesian segmentation of ultrasound imaging," *Ultrasonic Imaging*, vol. 17, pp. 291-304, 1995.
- [2] D. Boukerroui, O. Basset, A. Noble, and A. Baskurt, "Segmentation of ultrasound images - Multiresolution 2D and 3D algorithm based on global and local statistics," *Pattern Recognition Letters*, vol. 24, pp. 779-790, 2003.
- [3] K. Z. Abd-Elmoniem, A.-B. M. Youssef, and Y. M. Kadah, "Real time speckle reduction and coherence enhancement in Ultrasound imaging via nonlinear anisotropic diffusion," *IEEE Transactions on Biomedical Engineering*, vol. 49, pp. 997-1014, 2002.
- [4] Yongjian Yu and S. T. Acton, "Speckle reducing anisotropic diffusion," *IEEE Transaction on Image Processing*, vol. 11, pp. 1260-1270, 2002.
- [5] D. Comaniciu and P. Meer, "Mean shift analysis and applications," presented at Proceedings of the 1999 7th IEEE International Conference on Computer Vision (ICCV'99), Sep 20-Sep 27 1999, Kerkyra, Greece, 1999.
- [6] J. A. Jensen and P. Munk, "Computer Fantoms for Simulation Ultrasound B-mode and CFL Images," presented at 23rd Acoust. Imag. Symp., Boston, MA, 1997.
- [7] K. Fukunaga and L. D. Hostetler, "Estimation of the gradient of a density function with applications in pattern recognition.," vol. IT-21, pp. 32-40, 1975.
- [8] D. Comaniciu and P. Meer, "Mean shift: A robust approach toward feature space analysis," *IEEE Transactions on Pattern Analysis and Machine Intelligence*, vol. 24, pp. 603-619, 2002.
- [9] D. Comaniciu, V. Ramesh, and P. Meer, "The variable bandwidth mean shift and data-driven scale selection," presented at 8th International Conference on Computer Vision, Jul 9-12 2001, Vancouver, BC, 2001.
- [10] S. J. Sheather and M. C. Jones, "A reliable data-based bandwidth selection method for kernel estimation," *J.R. Statist. Soc. B*, vol. 53(3), pp. 683-690, 1991.

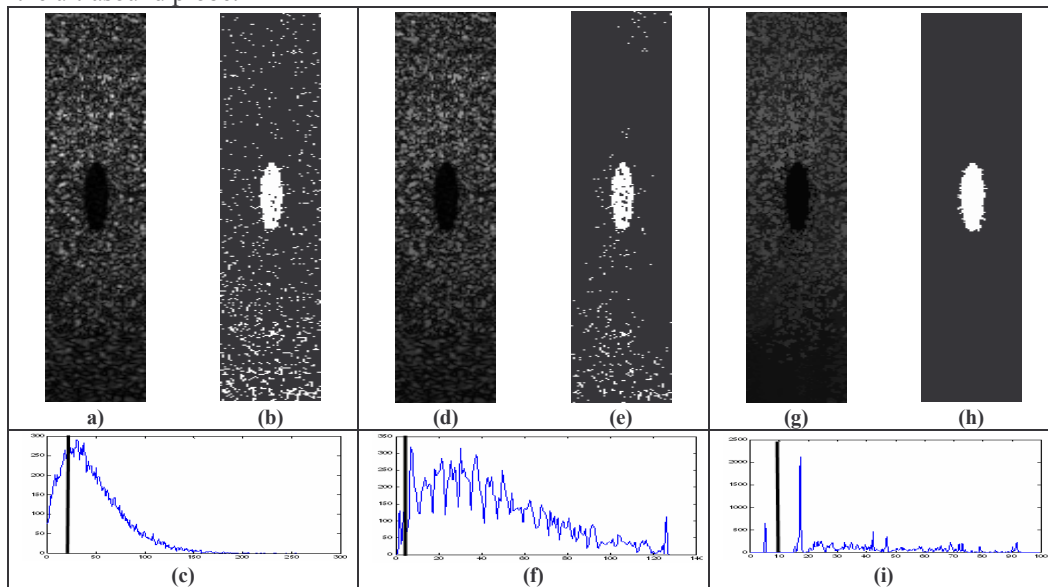


Figure 3: Results: a), b) original data and resulting manual thresholding; d), e) (VBMS R) filtered image and resulting manual thresholding; g), h) (VBMS R+S) filtered image and resulting automated thresholding; c), f), i) grey levels distributions of the images a), d) and g). The vertical lines indicate the threshold values.